



HAL
open science

Gas oversolubility in nanoconfined liquids: Review and perspectives for adsorbent design

Benoit Coasne, David Farrusseng

► To cite this version:

Benoit Coasne, David Farrusseng. Gas oversolubility in nanoconfined liquids: Review and perspectives for adsorbent design. *Microporous and Mesoporous Materials*, 2019, 288, pp.109561. 10.1016/j.micromeso.2019.109561 . hal-02328666

HAL Id: hal-02328666

<https://hal.science/hal-02328666v1>

Submitted on 5 Nov 2020

HAL is a multi-disciplinary open access archive for the deposit and dissemination of scientific research documents, whether they are published or not. The documents may come from teaching and research institutions in France or abroad, or from public or private research centers.

L'archive ouverte pluridisciplinaire **HAL**, est destinée au dépôt et à la diffusion de documents scientifiques de niveau recherche, publiés ou non, émanant des établissements d'enseignement et de recherche français ou étrangers, des laboratoires publics ou privés.

**Gas oversolubility in nanoconfined liquids:
review and perspectives for adsorbent design**

Benoit Coasne^{1,*} and David Farrusseng^{2,*}

¹ Univ. Grenoble Alpes, CNRS, LIPhy, Grenoble, France

² Université de Lyon, Université Claude Bernard Lyon 1, CNRS, IRCELYON - UMR
5256, Villeurbanne, France

* To whom correspondence should be addressed: Benoit Coasne (benoit.coasne@univ-grenoble-alpes.fr) and David Farrusseng (david.farrusseng@ircelyon.univ-lyon1.fr)

Abstract. Oversolubility effects refer to a large increase of the solubility of gases in liquids confined in nanoporous solids with respect to the value predicted by Henry's law. This review presents the state of the art of oversolubility by discussing the molecular mechanisms responsible for such effects and the conditions for their observation. Both experimental and theoretical approaches are reviewed, in a non-exhaustive fashion, with special emphasis on results that have helped to unravel the oversolubility phenomenon. Different porous materials including metal-organic frameworks (MOF), ordered porous silicas, and zeolites are considered in combination with various nanoconfined liquids and gases relevant to practical applications in energy and environmental science. Depending on the gas/liquid/solid system considered, oversolubility is shown to pertain either to adsorption (increased concentration at solid/gas and liquid/gas interfaces) or to confinement-induced solubility increase. We also critically discuss when oversolubility effects are expected to lead to improved performance in catalysis or environmental applications such as for air purification.

1. Introduction

The solubility of gases in liquids in the low pressure range can be described using Henry's law in which the concentration C of solubilized gas scales linearly with the gas partial pressure P . The proportionality factor k_H i.e. $C \sim k_H P$ is referred to as Henry's constant (Fig. 1) [1]. Henry's law can be derived as follows by starting from the equality of the gas fugacity f (or, equivalently, the gas chemical potential μ) in the gas phase and in the liquid phase: $f_g = f_l$ [2]. Under the assumption that the gas behaves as an ideal gas, $f_g = P$. As for f_l , we can write $f_l = \gamma(x) x f_l^{(0)}$ where γ is the activity coefficient, x is the mole fraction of gas molecules in the liquid, and $f_l^{(0)}$ is the fugacity of the liquid phase when it is only made of the gas molecules i.e. $x = 1$. Using a polynomial expansion for $\ln \gamma \sim a_1(1 - x) + a_2(1 - x)^2 + a_3(1 - x)^3 + \dots$, one recovers the two important asymptotic limits: (a) $\ln \gamma = 0$ for $x = 1$ as expected for a pure liquid for which $\gamma \sim 1$ and (b) $\ln \gamma \sim \text{constant}$ for $x \ll 1$. As a result, for $x \ll 1$, and noting that $C \sim x$, it is observed that Henry's law with $k_H \sim [\gamma f_l^{(0)}]^{-1}$ is a good approximation that describes the fugacity equality between the gas and liquid phases. In practice, the simple scaling between gas concentration and pressure in Henry's law holds provided that the gas partial pressure remains low enough and that the liquid does not chemically react with the solubilized gas.

For a given pressure P and temperature T , the gas solubility in liquids confined in large pores (typically, diameters D larger than a few nm) is identical or nearly identical to the bulk solubility taken under the same thermodynamic conditions. However, in the last decade, several experimental and theoretical studies have reported surprising results suggesting that, upon reduction of the liquid volume down to the *nm* scale by means of confinement in porous solids, a large gas solubility increase can be reached with respect to the predictions based on Henry's law (Fig. 1). Such enhanced solubility has been coined as "oversolubility". While the role of gas/solid interactions was identified as a key parameter, oversolubility in "nanoconfined liquids" was rapidly thought to be promoted by the layering of the liquid in the vicinity of the surface of the host porous solid. Such layering increases the overall solubility because of the confinement of gas molecules in the regions of low liquid density. However, enhanced gas solubility was also thought to be favored because of adsorption at the surface of the host porous material or at gas/liquid interfaces for incompletely filled pores.

Yet, despite the important studies dedicated to this intriguing phenomenon, the molecular origin of such gas oversolubility effects in liquids confined in nanoporous materials has been unraveled only recently. The emergence of a comprehensive and unifying picture of gas oversolubility in nanoconfined liquids is complex as it consists of triphasic systems where gas, liquid, and solid phases coexist. Such effects need to be better understood as they are relevant to important industrial processes related to energy and environmental sciences. These applications include but are not limited to three phase heterogeneous catalysis, oil and gas recovery, air purification, etc. While this point is not treated in detail here, oversolubility is also important for Earth science where the solubility of gases is expected to drastically affect both the retention and transport properties of geological media (see Ref. [3] for instance for a study on the solubility of small gases in clays).

In this paper, we review the state of the art on oversolubility effects observed when setting a gas in contact with nanoconfined liquids. By reviewing a non-exhaustive yet representative set of theoretical and experimental works on this topic, we discuss under which conditions such enhanced solubilities are observed and the underlying microscopic mechanisms. The remainder of this paper is organized as follows. In section 2, we present some key experimental and molecular simulation results which provide evidence for such oversolubility effects. In this section, it is also shown how these specific examples pertain to important energy and environment applications such as catalysis, carbon capture and storage and hydrogen storage and conversion. In section 3, we discuss the underlying microscopic mechanisms at the heart of oversolubility. We illustrate that oversolubility pertains either to an adsorption effect or to a confinement-induced solubility increase, and that the exact mechanism at play is governed by the ratio of the gas/solid to the liquid/solid interaction strengths. We also discuss in which conditions oversolubility leads to enhanced gas storage compared to adsorption and high-pressure processes.

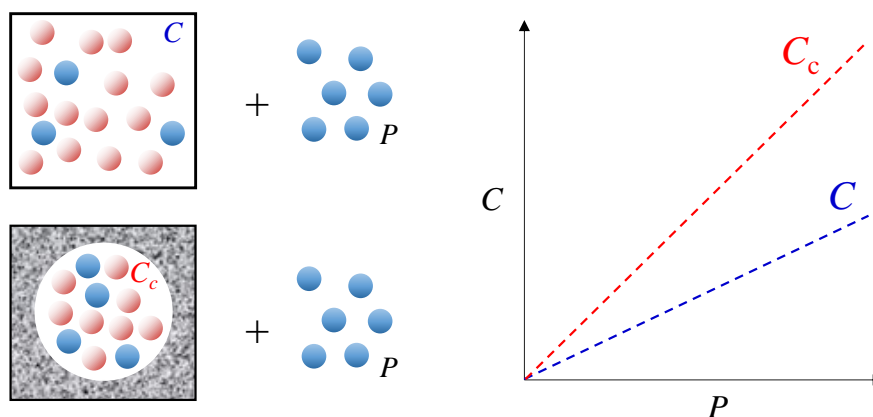


Fig. 1. Schematic representation of oversolubility effects in porous media. When gas molecules (blue spheres) at a pressure P are set in contact with a bulk liquid (red spheres), the concentration C of gas molecules solubilized in the liquid scales with the gas pressure, $C \sim k_H P$ where k_H is the so-called Henry constant. The latter relationship holds provided the pressure remains low enough (for higher pressures, non-linear relationships between C and P are observed). If the same gas is set in contact with the same liquid but confined in a porous material, the gas concentration C_c inside the porous material also depends linearly on pressure P at low pressures but large increases in the solubility can be observed.

2. Gas uptake in nanoconfined liquids

In this section, a few papers that have highlighted oversolubility effects in nanoconfined liquids are briefly reviewed. While the detailed microscopic picture of oversolubility in nanoconfined liquids will be given in the next section, the present section mainly focusses on reporting in a non exhaustive fashion some important oversolubility examples and their possible use for energy and environment applications (catalysis, carbon capture and storage and hydrogen storage and conversion).

Catalysis. From an experimental viewpoint, several accounts of gas oversolubility in nanoconfined liquids have been reported. In their pioneering work, Dalmon and coworkers reported a striking zero-order kinetics for hydrogenation when H_2 and liquid nitrobenzene are set into contact in a catalytic membrane [4]. Such an effect was discussed as the manifestation of an enhanced solubility phenomenon through which H_2 is solubilized in a large amount in the nanoconfined liquid. Later, using 1H -NMR, the same group confirmed this interpretation by

reporting evidence for large solubility enhancements for H₂ and light hydrocarbons (CH₄ and C₂H₆) in liquids such as CCl₄ and CS₂ confined in porous γ -alumina (pore size $D \sim 11$ nm) and silica (pore size $D \sim 13$ nm) [5]. In a series of papers, similar solubility enhancements were also observed using gas volumetric experiments for H₂ in several liquids confined in mesoporous solids with large pores such as γ -alumina and silica ($D > 10$ nm) but also with much smaller pores such as ordered porous silicas (MCM-41 with pores $D \sim 3$ -4 nm and SBA-15 with pores $D \sim 7$ nm), ordered porous aluminosilica (MCM-41 with Si/Al = 1 and pores $D \sim 3$ nm) and disordered porous silica (aerogel with pores $D \sim 9$ nm) [6,7,8].

Carbon capture and storage. Song and coworkers considered in a series of papers the use of an hybrid adsorbent, defined as a mesoporous silica filled with a liquid, to efficiently trap CO₂ [9,10,11]. Using polyethylenimine as liquid, these authors observed that the CO₂ adsorption capacity in the filled mesoporous silica is larger than that in the raw adsorbent (porous silica with no liquid) and that in pure polyethylenimine. In their experimental investigation, Song and coworkers also found that the loading has a strong impact on the oversolubility of CO₂ in polyethylenimine; In particular, an optimum was observed in the CO₂ solubility in the nanoconfined liquid when the liquid phase corresponds to 50 wt %. In line with these results on CO₂ capture, Ho et al. also reported experimental and molecular simulation results suggesting that nanoconfined liquids are efficient to trap large CO₂ amounts [12,13]. In particular, these authors found that the solubility of CO₂ in N-methyl-2-pyrrolydone (NMP) is increased by about a factor 6 when the liquid is confined in an ordered mesoporous silica (MCM-41 with a pore size $D \sim 3$ nm). In these two examples, the liquid does not chemically react with the solubilized gas *per se* but exhibits a medium strength acid-base interaction. In the case of water-CO₂ system, Soubeyrand-Lenoir et al. also reported a large increase by about a factor 5 of the CO₂ adsorption at a pressure of 0.2 bar in water confined in a MOF (Fe-MIL100 with pore size $D \sim 2$ -3 nm) [14].

H₂ storage. Hydrogen solubility in different porous materials filled with *n*-alkanes or ethanol was considered by Clauzier et al. [15,16]. Fig. 2 compares the H₂ solubility at room temperature in a Metal Organic Framework (MOF) and in an ordered mesoporous silica (MCM-41) filled with *n*-hexane (the fraction of porosity filled is 60%). The H₂ uptake in *n*-hexane confined in these two materials having a pore size of about $D \sim 3$ nm is found to be larger than the bulk

solubility in *n*-hexane and the adsorbed amount in the bare porous materials (i.e. when no liquid is adsorbed in the porosity). The fact that these two nanoporous materials have similar pore sizes show that the surface chemistry, porous volume and/or specific surface area are key parameters in describing oversolubility (in particular, considering that these materials have different pore geometries, the same pore size $D \sim 3$ nm does not necessarily correspond to the same specific surface to volume ratio or porous volume).

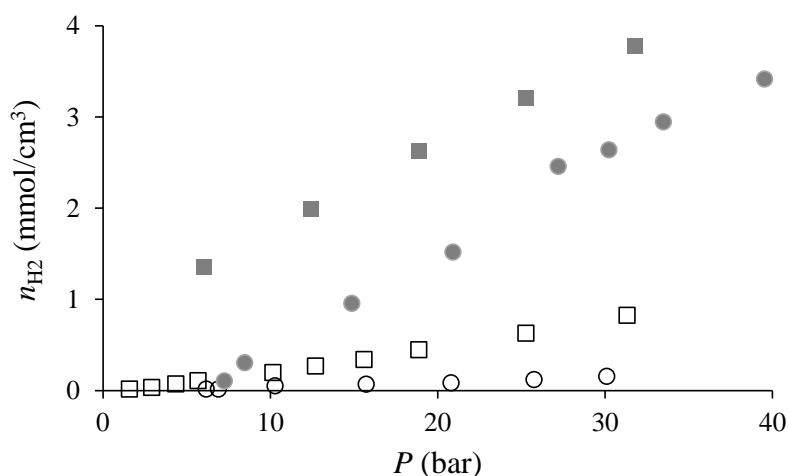


Fig. 2. Experimental H_2 uptake n_{H_2} in mmol/cm^3 of porous volume as a function of gas pressure P in bare porous materials (open symbols) and in porous materials that are 60% filled with *n*-hexane (closed symbols). The squares are for a metal organic framework (Cr-MIL101) while the circles are for an ordered porous silica (MCM-41). Both porous materials have a similar pore size $D \sim 3$ nm. The experimental temperature is $T = 298$ K. Adapted from Ref. [15].

The experiments on H_2 uptake in nanoconfined *n*-hexane shown in Fig. 2 was extended to other porous solids to include samples with larger pores (silica aerogel, $D \sim 10$ nm) and smaller pores (zeolite, $D \sim 1$ nm) [15]. Fig. 3 reports the H_2 solubility at $T \sim 298$ K and $P \sim 30$ bar in different porous solids as well as in the same porous solids that are 60% filled with *n*-hexane (for the sake of comparison, the H_2 solubility in bulk *n*-hexane is also shown). While the H_2 solubility in the microporous solid (zeolite, $D \sim 1$ nm) is similar to its bulk counterpart, large oversolubilities are observed when mesoporous solids are considered. Typically, when *n*-hexane is nanoconfined in a MOF, an oversolubility phenomenon is observed with a ~ 20 fold increase in the solubility compared to that in bulk *n*-hexane. Oversolubility is also observed for

other mesoporous solids (silica aerogel and MCM-41) although to a lesser extent. Interestingly, the fact that oversolubility is not observed for the material with ultrasmall pores (zeolite) suggests that the specific surface area is not the main parameter responsible for oversolubility and that there is an optimal pore size for maximum uptake. This result is fully consistent with previous conclusions by Song et al. and Ho et al. on CO₂ solubility in nanoconfined liquids (see above). In fact, as will be discussed in more details in the next section, the existence of an optimal pore size suggests that the pores must be large enough to allow for the layering of the liquid when nanoconfined (since confinement in subnanometric pores does not lead to strongly fluctuating density profiles due to severe curvature effects).

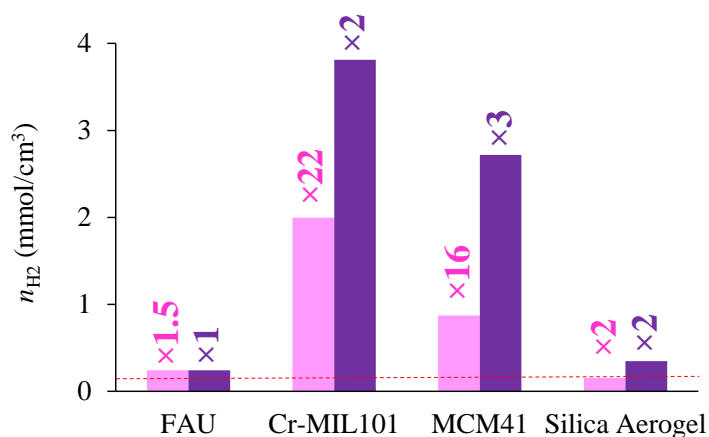


Fig. 3. Experimental H₂ uptake n_{H_2} at $T = 298$ K and $P = 30$ bar in mmol/cm³ in bare porous materials (pink) and in porous materials that are 60% filled with *n*-hexane (purple). The red dashed line indicates the solubility in bulk *n*-hexane under the same thermodynamic conditions. The porous materials considered are a zeolite (faujasite), a metal organic framework (Cr-MIL101), an ordered porous silica (MCM-41), and a disordered porous silica (aerogel). For each porous material, the two numbers indicate the H₂ uptake enhancement with respect to bulk *n*-hexane and with respect to the bare porous material, respectively. Adapted from Ref. [15].

3. Molecular mechanisms

Confinement and surface effects. Luzar and Bratko were the first to investigate the fundamental mechanisms for gas solubility in nanopores [17,18]. To assess the effect of

dissolved gases on the attractive force between hydrated hydrophobic surfaces, these authors considered the solubility of small inert gases such as O₂, N₂, CO₂ and Ar in water confined in hydrophobic nanopores with various sizes close to $D \sim 4$ nm. While Refs. [17,18] mainly focussed on the effect of gases on physical phenomena such as cavitation, hydrophobic attractive interactions in aqueous media, etc., important results were established such as an oversolubility by a factor from 5 to 10 for N₂ and O₂. The solubilized gases were found to be located at the pore hydrophobic surface (in between water and the pore surface). As a result, being a surface effect with no coupling induced from the correlations between opposite surfaces, oversolubility was thought in the work by Luzar and Bratko to scale with the specific surface area of the porous material. A few years after the papers by Luzar and Bratko, Ho et al. also carried a structural analysis of their molecular simulation data on CO₂ storage in nanoconfined liquids [12,13]. In addition to a non-negligible oversolubility effect, these atom-scale simulations suggested that the increased CO₂ solubility arises from the adsorption of CO₂ molecules into the cavities formed between the liquid molecules. Due to the packing of the liquid molecules close to the surface, the CO₂ molecules also form layers with an average density that exceeds the density reached when no liquid is confined in the porous material.

While the works cited above shed some light on oversolubility in a nanoconfined liquid, they do not provide a unifying picture for this complex phenomenon. These different studies show that the specific surface area of the porous material and nature of the interactions at play (solid/gas, liquid/gas, etc.) are key parameters but they do not establish the role of the different contributions: surface adsorption *versus* solubility within the confined solvent. In an effort to unravel the driving force and parameters for oversolubility, a molecular simulation study was carried out on the solubility of different gases – involving various interaction types – in water confined in several porous materials [19]. More in detail, the solubility S at $T = 298$ K was determined for N₂, CH₄, and CO₂ in water confined in a zeolite (Na-ZSM-5), an ordered porous silica (MCM-41), and a metal organic framework (MIL-100(Cr)) (Fig. 4). As shown in Fig. 4, an oversolubility effect was observed for all gas/solid couples considered since the gas solubility is larger at all pressures than the bulk solubility. To quantify the oversolubility phenomenon, Fig. 5 shows the so-called enhancement factor $s \sim S/S_0$ defined as the ratio of the gas solubilities in the confined S and bulk S_0 liquid (water). For all samples, it is observed that $f_{\text{CO}_2} < f_{\text{CH}_4} < f_{\text{N}_2}$ with f of the order of 10^0 to 10^3 depending on the porous material considered. While the results reported in Ref. [19] help understand the oversolubility mechanisms,

solubility in nanoconfined liquids was found to lead to lower storage capacity than achieved through direct physical adsorption in the different bare porous materials (i.e. with no confined liquid). Such a result can be explained by the pore volume reduction as the liquid occupies a non-negligible volume which becomes not accessible to the molecules in the gas phase. This point will be discussed in more detail below but the results in Ref. [19] are important as they suggest that oversolubility might not be as efficient as adsorption for capture and storage applications.

For all adsorbents, the solubility S within confined water follows the order $\text{CO}_2 \gg \text{CH}_4 > \text{N}_2$. Such an order can be explained by the strong quadrupole of CO_2 which leads to much stronger interaction with water than CH_4 and N_2 (see bulk data in Fig. 4 which suggests that the bulk solubility also follows the order $\text{CO}_2 \gg \text{CH}_4 > \text{N}_2$). For each gas, the solubility S within confined water follows the order: $\text{ZSM-5} < \text{MCM-41} < \text{MIL-100}$. Such an order can be correlated to the pore volume or specific surface area which also follows the same order $\text{ZSM-5} < \text{MCM-41} < \text{MIL-100}$.

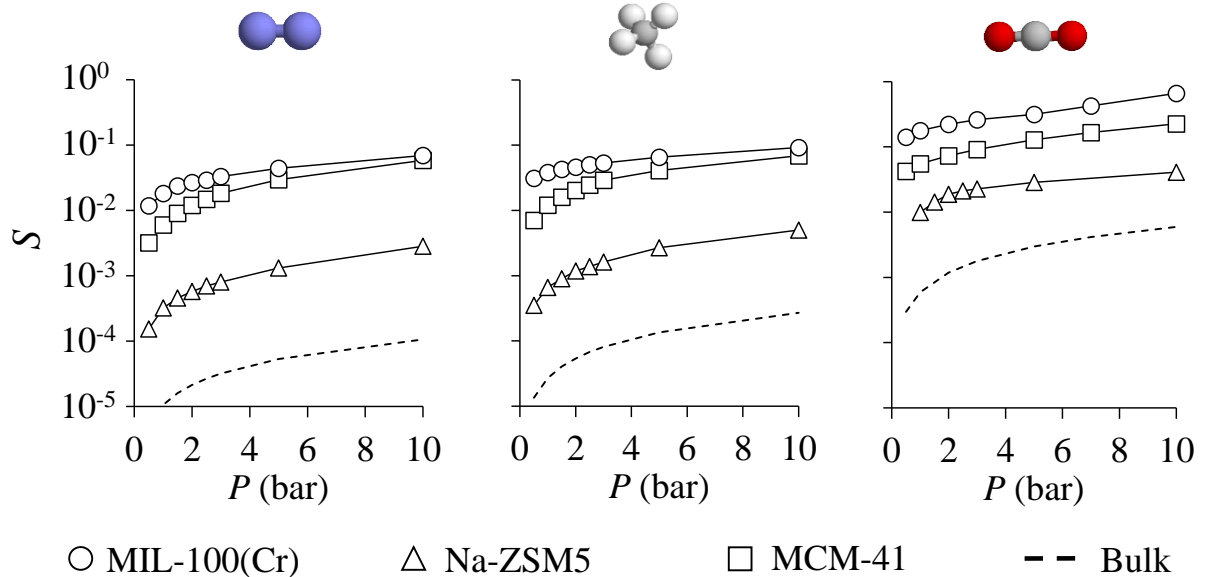


Fig. 4. Simulated solubility S at $T = 298$ K for N_2 , CH_4 , and CO_2 in a porous material filled with water. S is expressed as a dimensionless value which corresponds to a number of moles of gas per mole of water. The triangles, squares, and circles are for a zeolite (Na-ZSM-5), an ordered porous silica (MCM-41), and a metal organic framework (MIL-100(Cr)). The dashed line corresponds to the simulated solubility for bulk water, S_0 . Adapted from Ref. [19].

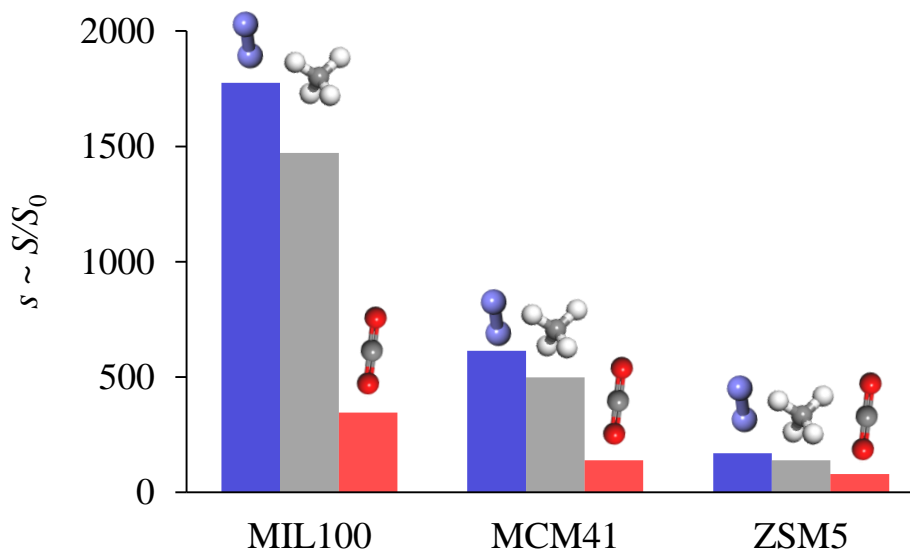


Fig. 5. Simulated solubility enhancement, $s = S/S_0$, at $P = 1$ bar and $T = 298$ K bar for CO₂, CH₄, and N₂ in a porous material filled with water: zeolite (Na-ZSM-5), ordered porous silica (MCM-41), and metal organic framework (MIL-100(Cr)). Adapted from Ref. [19].

Adsorption versus solubility. As recently illustrated by Gadikota et al. [3], understanding the selectivity and solubility of gases in nanoconfined liquids require the estimation of the free enthalpy variation ΔG upon transferring (or exchanging) a gas molecule from the bulk to the confined phase. Here, the free enthalpy must be considered as the relevant thermodynamic potential because the transfer occurs at constant temperature and pressure. In their work on small inert gases in hydrated minerals (clays), Gadikota et al. found that, as expected, gas solubility in nanoconfined water strongly depends on the size and shape of the gas molecule. While molecular dynamics can be used to assess ΔG for different gases, liquids and solids, its experimental determination appears to be more complicated although doable. In what follows, we show that oversolubility as well as the underlying microscopic mechanism (i.e. adsorption *versus* solubility) can be anticipated based on simple parameters such as the characteristic strength of the gas/solid, ϵ_{GS} , and liquid/solid, ϵ_{LS} , interactions (which directly correlate to the experimental heats of adsorption for the gas and liquid, $\epsilon_{GS} \sim \Delta H_{\text{ads}[G]}$ and $\epsilon_{LS} \sim \Delta H_{\text{ads}[L]}$).

To disentangle surface *versus* volume effects in oversolubility, Coasne and coworkers [20] carried out a molecular simulation on CO₂ and H₂ solubility in a simple liquid (OMCTS = octamethylcyclotetrasiloxane) confined in an ordered mesoporous silica (MCM-41, $D \sim 3$ nm).

These two gases were selected in combination with hydroxylated silica as they are prototypical of strongly and weakly interacting gases, respectively. Considering the typical interactions between OMCTS and the silica surface, $\epsilon_{GS} > \epsilon_{LS}$ for CO_2 and $\epsilon_{GS} \ll \epsilon_{LS}$ for H_2 since the different enthalpies of adsorption for CO_2 , H_2 and OMCTS in hydroxylated silica are $\Delta H \sim 34$, ~ 8 , and ~ 22 kJ/mol, respectively. As shown in Fig. 6, for all pressures, the CO_2 and H_2 solubilities at 298 K in the bulk and confined liquid are larger than their bulk counterpart. As expected, the CO_2 solubility data show larger uptakes than H_2 due to the stronger interaction of CO_2 with both the solid and liquid. Interestingly, the solubility for these two gases when the pore is incompletely filled – with only one adsorbed OMCTS layer formed at the pore surface – is even larger than the solubility for the completely filled pore. This result already points out to an important contribution arising from adsorption at gas/liquid interfaces. In this respect, although gas adsorption at gas/liquid interfaces located at the external surface of porous materials can lead to oversolubility, this contribution is expected to be negligible since most porous materials exhibit very small external surfaces. On the other hand, when the gas/liquid interface is located inside the pore (incomplete filling prior to liquid capillary condensation), oversolubility arising from adsorption at gas/liquid interfaces is expected to be non-negligible.

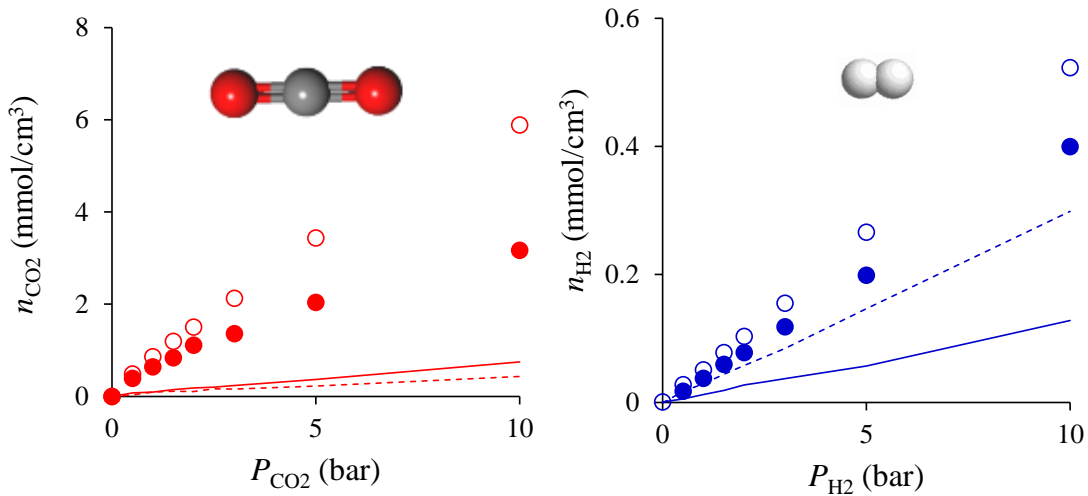


Fig. 6. Simulated gas uptake, n_{CO_2} and n_{H_2} , in mmol per cm^3 at $T = 298$ K as a function of pressure for CO_2 (left) and H_2 (right) in an ordered porous silica (MCM-41): filled with one layer of OMCTS (open circles) and fully filled with OMCTS (closed circles). The bulk gas density (dashed line) and gas solubility in bulk OMCTS (solid line) are also shown. Adapted from Ref. [20].

To identify the molecular mechanisms responsible for oversolubility, Fig. 7 shows the density $\rho(r)$ as a function of the position r with respect to the silica pore center ($r = 0$) for CO₂, H₂, and OMCTS at room temperature and a pressure $P = 1$ bar (both complete and incomplete pore fillings by the liquid are shown). As expected, the liquid forms layers in the vicinity of the surface with marked density oscillations which smear out as the liquid molecules get adsorbed further away from the surface. Regardless of the pore filling, CO₂ is preferentially adsorbed at the silica surface due to its strong interaction with the hydroxylated silica (CO₂ quadrupole with OH dipole) while H₂ is not located in the vicinity of the silica surface but present in regions of low liquid density. The thickness of the CO₂ adsorbed film, located between the silica surface and the first adsorbed OMCTS layer, increases with pressure. H₂ is found in the pore center in regions of low OMCTS density. These results confirm that the ratio of the solid/gas to the solid/liquid interaction strengths drives the oversolubility phenomenon. On the one hand, oversolubility is an adsorption-driven mechanism for $\epsilon_{GS} > \epsilon_{LS}$ (e.g. CO₂/OMCTS/silica). On the other hand, oversolubility is a confinement-induced enhanced solubility mechanism for $\epsilon_{GS} < \epsilon_{LS}$ (e.g. H₂/OMCTS/silica). This interpretation is consistent with the results from Ref. [19] discussed above regarding the solubility of CO₂, CH₄, and N₂ solubility in water confined in zeolite, ordered porous silica, and metal organic framework. For all these systems, owing to the strong interaction between water and the host porous material, we can safely assume that $\epsilon_{GS} < \epsilon_{LS}$ so that oversolubility is expected to be a confinement-induced oversolubility effect.

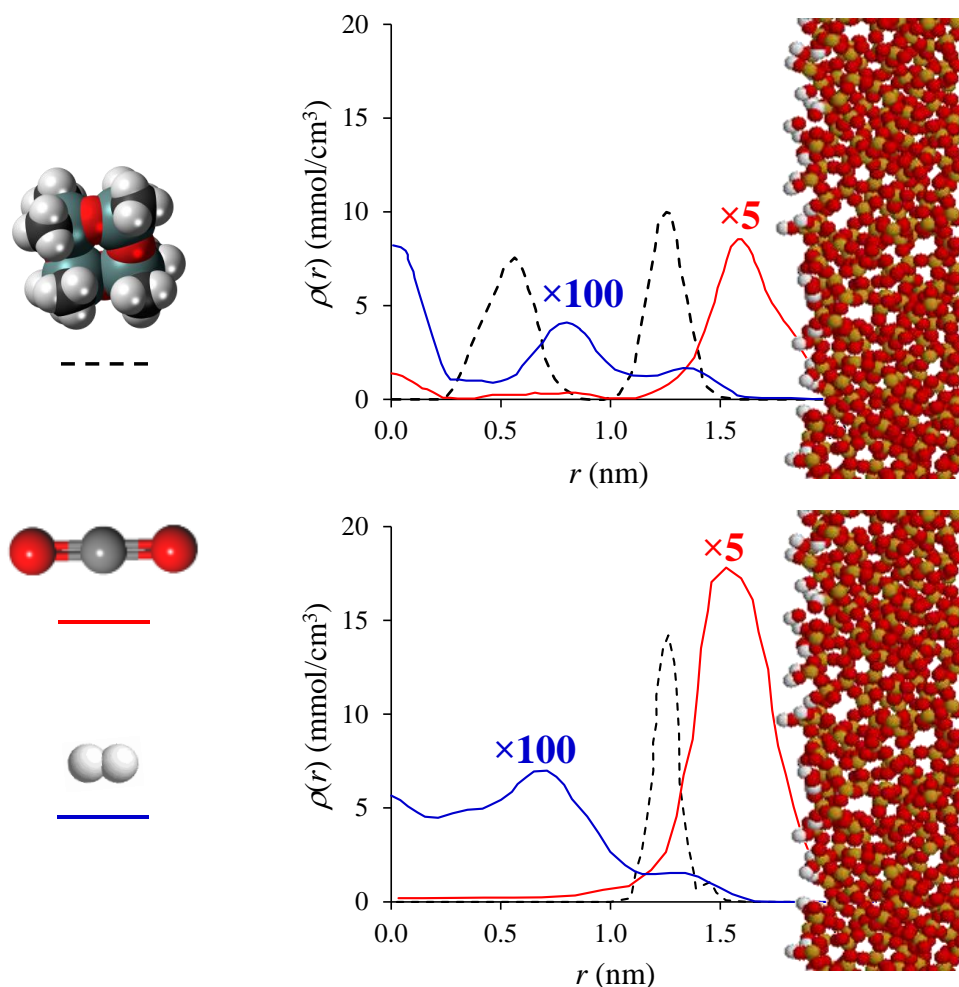


Fig. 7. Simulated density profiles at $T = 298$ K and $P = 1$ bar for CO_2 (red) and H_2 (blue) in an ordered porous silica (MCM-41): filled with one layer of OMCTS (*bottom*) and fully filled with OMCTS (*top*). The black dashed lines indicate the density profiles for the liquid OMCTS for CO_2 (similar OMCTS profiles were found for H_2). For the sake of clarity, the density for CO_2 and H_2 have been multiplied by $\times 5$ and $\times 100$, respectively. The position of the hydroxylated silica surface is shown (oxygen, hydrogen and silicon atoms correspond to the red, white and orange spheres). Adapted from Ref. [20].

In Ref. [20], in addition to a simple criterion based on the comparison of the gas and liquid heats of adsorption, a simple model was proposed to assess whether oversolubility in a nanoconfined liquid corresponds to an adsorption or a bulk-like solubility mechanism. In this method, one estimates the expected solubility $S_0(r)$ at a distance r from the silica pore center ($r = 0$); $S_0(r)$ is defined as the bulk solubility $S_{\text{bulk}}[\rho = \rho_{\text{liquid}}(r)]$ taken at the liquid density ρ corresponding to the density $\rho_{\text{liquid}}(r)$ of the liquid at the position r within the pore. Fig. 8

illustrates how $S_0(r)$ can be estimated using Monte Carlo simulations in the Grand Canonical ensemble for different bulk liquid densities. By comparing the measured local solubility $S(r)$ with $S_0(r)$, one can assess whether oversolubility pertains to adsorption or solubility. On the one hand, if $S(r) = S_0(r)$, oversolubility is a bulk-like solubility phenomenon where the solubility is enhanced because of the large density fluctuations in the nanoconfined liquid. On the other hand, if $S(r) \neq S_0(r)$, adsorption effects can be identified and quantified.

Fig. 9 compares the simulated $S(r)$ and expected $S_0(r)$ solubility profiles for CO₂ and H₂ in OMCTS nanoconfined in the silica pore (MCM-41, $D \sim 3$ nm). As expected, $S(r)$ for H₂ is very close to $S_0(r)$ because H₂ oversolubility pertains to a bulk-like solubility mechanism. This confirms that the solubility enhancement for H₂ occurs in the low liquid density regions induced by the significant layering of the confined liquid. In the pore center, $S(r)$ for CO₂ matches $S_0(r)$ because CO₂ solubility far from the solid surface also pertains to a solubility mechanism (because of vanishing surface/gas interactions as $r \rightarrow 0$). However, in the vicinity of the pore surface, CO₂ oversolubility is an adsorption-driven mechanism as departure between $S(r)$ and $S_0(r)$ is observed.

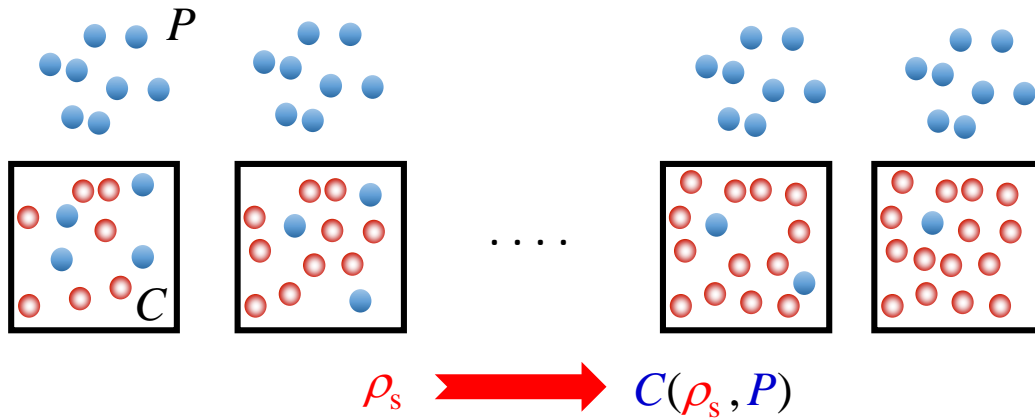


Fig. 8. Principle of the molecular simulations used to determine the bulk solubility of a gas as a function of the liquid density ρ_s for CO₂ and H₂. The blue and red spheres denote the gas (solute) and liquid (solvent) molecules, respectively. For different liquid densities, the concentration $C(\rho_s, P)$ of gas molecules is determined using Grand Canonical Monte Carlo simulations as a function of pressure P (which is obtained from the chemical potential μ). The solubility $S_{\text{bulk}}[\rho_s]$ is simply defined as the ratio of the gas and liquid densities as a function of the liquid density ρ_s .

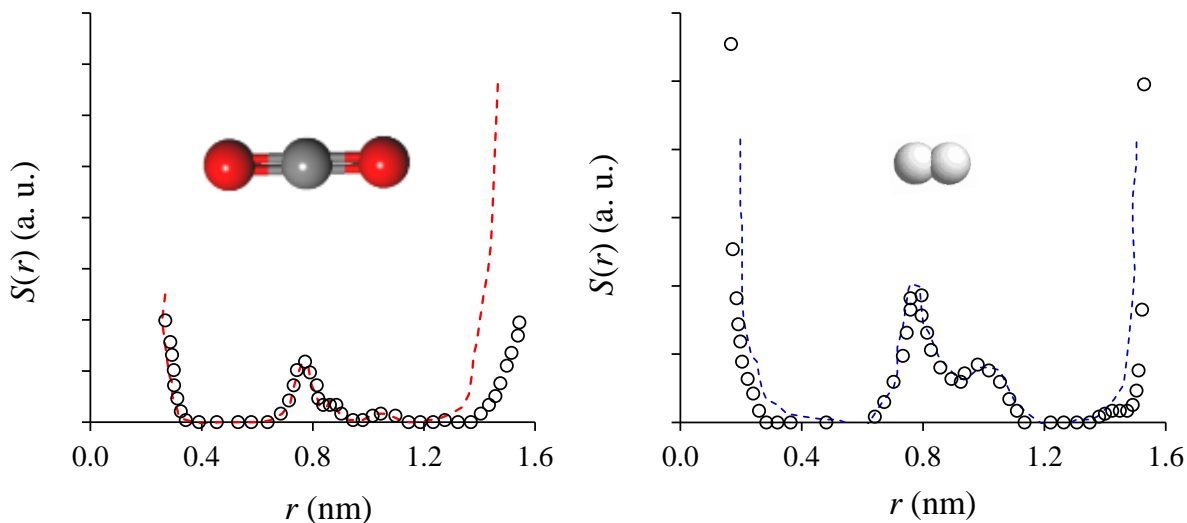


Fig. 9. Comparison between the simulated solubility profile $S(r)$ (symbols) and the expected solubility $S_0(r)$ (dashed line) for CO_2 (left) and H_2 (right) in a MCM-41 silica pore. The temperature and pressure are $T = 298$ K and $P = 1$ bar, respectively. The expected solubility is defined as $S_0(r) = S_{\text{bulk}}[\rho = \rho_{\text{liquid}}(r)]$ where S_{bulk} is the bulk solubility at a density ρ equal to the local density $\rho_{\text{solvent}}(r)$. Adapted from Ref. [20].

Temperature effect. A simple microscopic picture has emerged from the reviewed works above. Oversolubility is either an adsorption (surface) or a solubility (volume) phenomenon. The comparison between the gas/solid, ϵ_{GS} , and liquid/solid, ϵ_{LS} , interaction strengths, which can be estimated from the corresponding differential heats of adsorption, can be used to predict the type of oversolubility expected for a given gas/liquid/solid system. Yet, some important questions remain to be addressed such as the role of temperature. While the criterion relying on the interaction strengths is expected to apply at any temperature, the interpretation of data on oversolubility as a function of temperature often proves to be non-trivial. Adsorption-driven oversolubility must decrease with temperature as physical adsorption is exothermic; as a result, for $\epsilon_{\text{GS}} > \epsilon_{\text{LS}}$, oversolubility should decay with temperature as gas adsorption close to the pore surface becomes less significant. The qualitative temperature dependence of confinement-induced enhanced solubility is more complicated to anticipate as it involves both entropy and energy contributions (like bulk solubility). While the energy contribution to confinement-induced enhanced solubility is also expected to decrease with increasing temperature, the

entropy contribution is expected to increase with increasing temperature. The situation is even more complex as the effect of temperature on layering – responsible for confinement-induced enhanced solubility – results from competitive mechanisms; increasing the temperature will lead at the same time to larger density fluctuations in the confined liquid but less pronounced layering.

This complexity is well illustrated by the data from Clauzier et al. on the the temperature dependence of H₂ solubilized in different *n*-alkanes confined in a silica aerogel ($D \sim 10$ nm) [16]. The H₂ uptake was found to increase upon increasing the temperature so that the authors concluded that the entropy contribution to such confinement-induced oversolubility dominates. In other words, upon increasing the temperature, the increased flexibility and conformation of the confined *n*-alkane molecules generate large and numerous subnanometric cavities that solubilize a great amount of H₂ molecules. However, for a given temperature and pressure, the H₂ oversolubility was found to increase with decreasing the alkane chain length – a result that seems to contradict the entropy-driven picture inferred from the temperature dependence (entropy effects are necessarily more important for long molecules than for short molecules). As explained in Ref. [16], all these results can be rationalized by considering the number density ρ_C of CH_{*x*} (*x* = 2 or 3) groups instead of the number density ρ_M of alkane molecules. At a given temperature *T*, ρ_C decreases upon decreasing the alkane chain length so that the free volume increases and, therefore, allows solubilizing a larger number of H₂ molecules.

As another illustration of the complex temperature dependence of oversolubility, Song et al. showed that CO₂ oversolubility in polyethylenimine nanoconfined in MCM-41 increases with increasing the temperature (like for CO₂ solubility in bulk polyethylenimine) [9,10,11]. While further study is needed to clarify this result, the authors interpreted the temperature dependence as a kinetic issue. Independently of the polyethylenimine packing and conformation within the porous silica, diffusivity of CO₂ towards the nitrogen atoms (active sites in polyethylenimine) increases with temperature so that CO₂ trapping appears more efficient at high temperature than at low temperature. The effect of temperature on gas uptake can provide an indication of the uptake mechanism at play in gas/solid/liquid triphasic systems. However, even when the enthalpies of adsorption and solubility are very different, such a temperature influence may remain somewhat non-conclusive. Taking the system CO₂/water/13X zeolite as an illustrative

example (Fig. 10) [21,22], while the heat of CO₂ adsorption in 13X zeolite (−45 kJ/mol) is significantly larger than the heat of solubilization (−20 kJ/mol), experimental data obtained upon increasing the temperature from 30 to 60°C at pressures above 10 bar do not provide a clear answer regarding the efficiency of adsorption *versus* solubility mechanisms; the adsorbed amount decreases by 20% while the solubilized amount decrease by 50% for the dissolution. This example illustrates that experimental conditions must be carefully chosen based on the data for the corresponding binary systems (gas/solid and gas/liquid) to identify pressure and temperature ranges where the temperature evolution departs significantly.

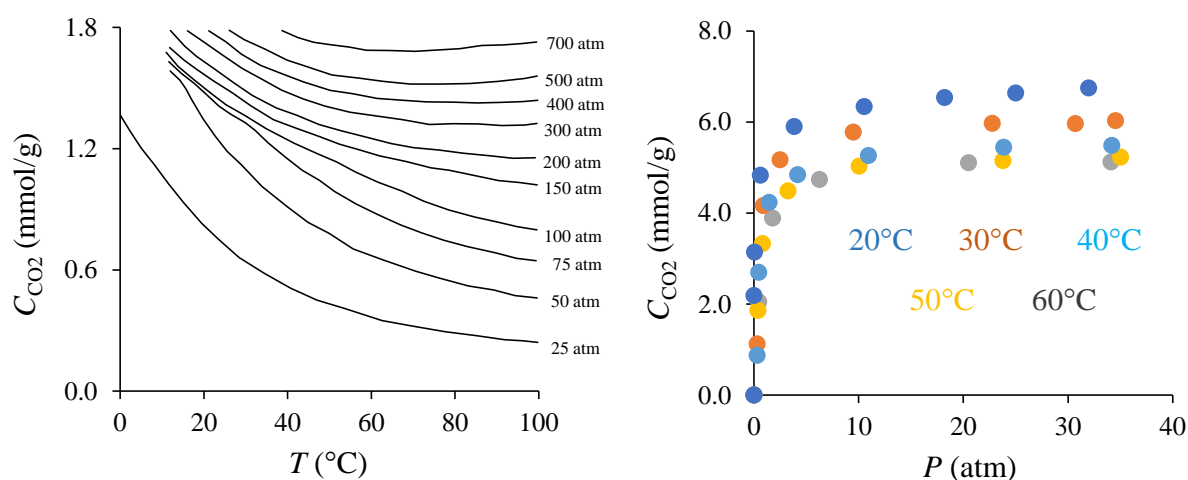


Fig. 10. (left) Solubility $C_{CO_2}(T, P)$ as a function of temperature at different pressures P for CO₂ in bulk water. (right) Adsorption isotherms for CO₂ in a zeolite 13X at different temperatures from 20°C to 60°C. Adapted from Refs. [21,22].

4. Conclusion and perspectives

In this review, the microscopic origins of enhanced gas solubility in nanoconfined liquids, also known as “oversolubility”, were discussed in the light of available experimental and theoretical data. Depending on the liquid/gas/porous solid triphasic system considered, oversolubility is an adsorption effect or a confinement-induced solubility enhancement. On the one hand, for gas/adsorbent interactions stronger than the liquid/solid interactions, the gas uptake corresponds to an adsorption-driven effect as the gas molecules get adsorbed between the solid surface and the nanoconfined liquid. On the other hand, for gas/solid interactions weaker than the liquid/solid interactions, the gas uptake corresponds to a confinement-induced enhanced solubility with the solubility being favored in the low solvent density regions. In porous solids that are partially filled by the liquid, the gas uptake is further increased because of adsorption

at the gas/liquid interface. These findings pave the way for the rational design of novel hybrid adsorbents in the context of gas capture, catalysis, phase separation, etc. In particular, the fundamental understanding of the different molecular mechanisms leading to oversolubility provides a unified framework to predict and design optimal adsorbents and processes (including adequate temperature and pressure conditions) using readily available parameters (surface chemistry, pore size, heat of adsorption, adsorbate capacity, solubility, etc.).

Oversolubility as a mean to increase local gas densities in separation and catalytic processes has not been considered in the literature. In particular, despite being a promising tool to increase process efficiency by controlling the local thermodynamics, no attempt has been made to optimize this effect and its influence on a given application. However, while oversolubility is expected to lead to potential benefits in optimizing adsorbent-based processes in triphasic systems, there are a number of applications where simple adsorption (i.e. with no confined liquid) in a porous medium will largely surpass oversolubility. This includes several gas storage applications such as H₂ and CO₂ where the presence of the liquid is actually detrimental to the maximum storage capacity (as the confined liquid occupies the porosity so that the volume available for gas storage is decreased). For example, in the case of the triphasic system CO₂/water/13X zeolite considered above, the solubility of CO₂ in water at 1 bar and room temperature is 34 mol/m³ while CO₂ adsorption in 13X zeolite ~4000 mol/m³ is two orders of magnitude larger (in this estimate a zeolite apparent density of 1 g/cm³ was used). A second example is the triphasic system Xe/hydrocarbon/active carbon which can be considered for noble gas recovery application from nuclear fission products – an important concern with economical and environmental impacts. In the specific case of Xe capture, adsorption at a pressure of 1 bar of Xe in contact with an active carbon is 0.01 mol/g which leads to 5000 mol/m³ (an apparent density of 0.5 g/cm³ is used for the active carbon) [23]. In contrast, the solubility of Xe in hydrocarbon at a Xe pressure of 1 bar is ~ 140 mol/m³ [24] which is about more than one order of magnitude lower than the value obtained using adsorption.

In contrast to the gas storage/separation applications above, there is a number of applications where oversolubility is expected to be beneficial in terms of process efficiency. This is particularly true for triphasic heterogenous catalytic processes using microporous catalysts or support. This includes hydrocracking of hydrocarbons for refinery applications but also aqueous phase catalytic oxidation for environmental applications. CO₂-based enhanced oil

recovery could also be optimized using oversolubility effects by modifying the thermodynamic equilibrium between solubilized gases in complex liquid (aqueous) mixtures trapped in the porosity of rocks. A better understanding of the oversolubility mechanisms will also facilitate the design of performing porous adsorbents for air purification – especially for volatile organic compounds (VOCs) – which is a major societal concern. In ambient conditions, i.e. with relative humidities ranging from 40 to 95%, the surface of porous solids, especially microporous solids, is covered by a layer of water molecules or even filled with water. Considering that the solubility of VOCs in water depend very much on their nature, oversolubility could be used to optimize and improve their purification using porous adsorbents. As an illustration, short aldehydes such as formaldehydes and acetaldehydes solubilize very well in water while benzene, toluene and xylenes (BTX) and larger polyaromatics do not. For each of these system types, and depending on the porous adsorbent considered, either adsorption-driven or solubility-driven oversolubility could be used to design novel purification units.

Acknowledgments. Part of this work was supported by a grant from the Project OCTAPPOM within the research program NEEDS (Nucléaire, Energie, Environnement, Déchets et Société).

References

-
- [1] W. Henry, *Phil. Trans. R. Soc. London* 93 (1803) 29–274.
 - [2] J. M. Prausnitz, R. N. Lichtenthaler, E. Gomes de Azevedo, *Molecular thermodynamics of fluid phase equilibria* (3rd edition), Prentice Hall PTR, Upper Saddle River, NJ, USA (1999).
 - [3] G. Gadikota, B. Dazas, G. Rother, M. C. Cheshire, I. C. Bourg, *J. Phys. Chem. C* 121 (2017) 121 26539–26550.
 - [4] J. Peureux, M. Torres, H. Mozzanega, A. Giroir-Fendler, J. A. Dalmon, *Catal. Today* 25 (1995) 409–415.
 - [5] S. Miachon, V. V. Syakaev, A. M. Rakhmatullin, M. Pera-Titus, S. Caldarelli, J. A. Dalmon, *ChemPhysChem* 9 (2008) 78–82.
 - [6] M. Pera-Titus, R. El-Chahal, V. Rakotovao, C. Daniel, S. Miachon, J. A. Dalmon, *ChemPhysChem* 10 (2009) 2082–2089.
 - [7] M. Pera-Titus, S. Miachon, J. A. Dalmon, *AIChE J.* 55 (2009) 434–441.
 - [8] V. Rakotovao, R. Ammar, S. Miachon, M. Pera-Titus, *Chem. Phys. Lett.* 485 (2010) 299–303.

-
- [9] C. S. Song, *Catal. Today* 115 (2006) 2–32.
- [10] X. C. Xu, C. S. Song, B. G. Miller, A. W. Scaroni, *Fuel Chemistry* 49 (2004) 300–301.
- [11] X. C. Xu, C. S. Song, B. G. Miller, A. W. Scaroni, *Ind. Eng. Chem.* 44 (2005) 8113–8119.
- [12] L. N. Ho, J. P. Perez, F. Porcheron, R. J. M. Pellenq, *Langmuir* 27 (2011) 8187–8197.
- [13] L. N. Ho, J. P. Perez, F. Porcheron, R. J. M. Pellenq, *J. Phys. Chem. C* 116 (2012) 3600–3607.
- [14] E. Soubeyrand-Lenoir, C. Vagner, J. W. Yoon, P. Bazin, F. Ragon, Y. K. Hwang, C. Serre, J. S. Chang, P. L. Llewellyn, *J. Am. Chem. Soc.* 134 (2012) 10174–10181.
- [15] S. Clauzier, L. N. Ho, M. Pera-Titus, B. Coasne, D. Farrusseng, *J. Am. Chem. Soc.* 134 (2012) 17369–17371.
- [16] S. Clauzier, L. N. Ho, M. Pera-Titus, D. Farrusseng, B. Coasne, *J. Phys. Chem. C* 118 (2014) 10720–10727.
- [17] A. Luzar, D. Bratko, *J. Phys. Chem. B* 109 (2005) 22545–22552.
- [18] D. Bratko, A. Luzar, *Langmuir* 24 (2008) 1247–1253.
- [19] L. N. Ho, Y. Schuurman, D. Farrusseng, B. Coasne, *J. Phys. Chem. C* 119 (2015) 21547–21554.
- [20] L. N. Ho, S. Clauzier, Y. Schuurman, D. Farrusseng, B. Coasne, *J. Phys. Chem. Lett.* 4 (2013) 4, 2274–2278.
- [21] R. Saskatchewan, *Equilibrium and mass transfer behaviour of CO₂ adsorption on zeolites, carbon molecular sieve, and activated carbons*, PhD Thesis, University of Regina (2012).
- [22] R. Wiebe, V. L. Gaddy, *J. Am. Chem. Soc.* 62 (1940) 815–817.
- [23] K. Munakata, T. Fukumatsu, S. Yamatsuki, K. Tanaka, M. Nishikawa, *J. Nucl. Sci. Tech.* 36 (1999), 818–829.
- [24] M. Steinberg, B. Manowitz, *Nucl. Technology* 51 (1959) 47–50.